Propagating Fronts and Chaotic Dynamics in $Co(OH)_2$ Liesegang Systems

V. Nasreddine and R. Sultan*

Department of Chemistry, American University of Beirut, Beirut, Lebanon

Received: November 11, 1998

This paper presents a study of some features and characteristics of the Co^{2+}/NH_4OH Liesegang system. The pattern of parallel $Co(OH)_2$ bands displays peculiar properties that are unique among other Liesegang systems. First, the process of dissolution of bands at the top of the pattern coupled to the formation of new ones at the bottom results in a propagating pattern that moves down the tube. Second, the total number of bands *N* varies erratically with time, unlike other Liesegang systems in which *N* increases monotonically with time. These random oscillations in the variable *N* are related to the dissolution/precipitation scenario. New experiments are designed to obtain a rigorous measurement of the total number of bands. Image analysis software (SigmaScan) is used to accurately determine *N* and the distance of the first band from the junction between the two solutions, based on a cutoff zero absorbance criterion. A time series for *N* is obtained by monitoring the pattern for 40 consecutive days. This time series is then analyzed numerically using a "Chaos Data Analyzer" software. All the characterization tools (such as power spectra, phase portraits, Lyapunov exponents and fractal dimensions) suggest a chaotic behavior of deterministic nature. The distance of the first band from the interface is plotted versus time. The velocity of dissolution is determined by obtaining a functional fit from the time variation curve and then calculating a derivative curve of that fit. The derivative is particularly evaluated at $t = 10$ and 15 days (taken as reference days), thus yielding the velocity of the dissolution front. A similar method is used for the distance of the last band from the interface, to determine the velocity of the precipitation front. The measurements are performed for five different concentrations (*C*) of cobalt chloride and the dependence of the two front velocities on *C* is investigated. Both front velocities are found to decrease monotonically with increasing *C* with a linear correlation existing between them.

1. Introduction

In an earlier work[1] on the features of $Co(OH)_2$ Liesegang[2−5] patterns (from Co^{2+} and NH_4 OH in gelatin), we found that the total number of bands (*N*) shows a random variation with time. This is different from most other Liesegang systems where *N* increases monotonically with time.[6] This behavior is due to a scenario of band dissolution and band formation yielding an oscillatory variation of *N*. By carrying out new experiments, we establish that the band dissolution occurs at the top of the pattern, accompanied by the precipitation of new bands at the bottom, thus causing the whole pattern to propagate down the tube. This observed migration of the pattern and the erratic time variation of *N* appear to be two coupled phenomena, suggesting the possibility of deterministic chaos inherent in the dynamics of the system.

The present paper is concerned with the explanation of the observed behavior and its characterization as either deterministic chaotic (being an intrinsic property of the reaction−diffusion processes) or stochastic (resulting from random fluctuations). The observed oscillatory behavior is not in conformity with a typical Liesegang patterning experiment where the total number of bands increases monotonically with time. The latter traditional behavior is seen notably in systems such as $AgNO_3/K_2CrO_4$,[6,7] $MgCl_2/NH_4OH$,[8] and $Pb(NO_3)_2/KI$[9]. This notable difference distinguishes the Co^{2+}/NH_4OH system from other systems and makes it particularly interesting for further investigation. The variable *N* is found to behave chaotically for a range of $CoCl_2$ concentrations tested. The precipitation reaction is

$$CoCl_2(aq) + 2NH_4OH(aq) \rightleftharpoons Co(OH)_2(s) + 2NH_4Cl(aq)$$

Although the propagation of the pattern down the tube is not a typical property of a Liesegang system, it nevertheless reproduces previous observations on precipitation reactions in gelled media, notably in the $Cr(OH)_3$[10] and the HgI_2[11] systems. The latter, however, exhibit the propagation of a single band instead of a stratum of parallel bands. The dissolution of the bands at the top of the tube and the formation of new ones at the bottom is a property of the system dynamics and is apparently responsible for the observed chaotic variation in the number of bands. Note that the band dissolution is due to complex formation in an excess of NH_4Cl,[12,13] according to the reaction

$$Co(OH)_2(s) + 6NH_4Cl(aq) \rightleftharpoons [Co(NH_3)_6]Cl_2(aq) + 4HCl(aq) + 2H_2O$$

A systematic study will be performed here to monitor the random variation of the quantity *N* over relatively long periods of time and to characterize it as deterministic chaos or a result of random fluctuations, according to existing standard methods.[14,15] A method of measurement of the front velocities for dissolution and precipitation will also be advanced.

2. Experimental Section

2.1. Pattern Preparation and Monitoring. A gel solution (Difco gelatin, 1%) of $CoCl_2$ is placed in a set of thin tubes (of

* To whom correspondence should be addressed. E-mail: rsultan@aub.edu.lb.

10.1021/jp984392w CCC: $18.00
Published on Web 04/01/1999

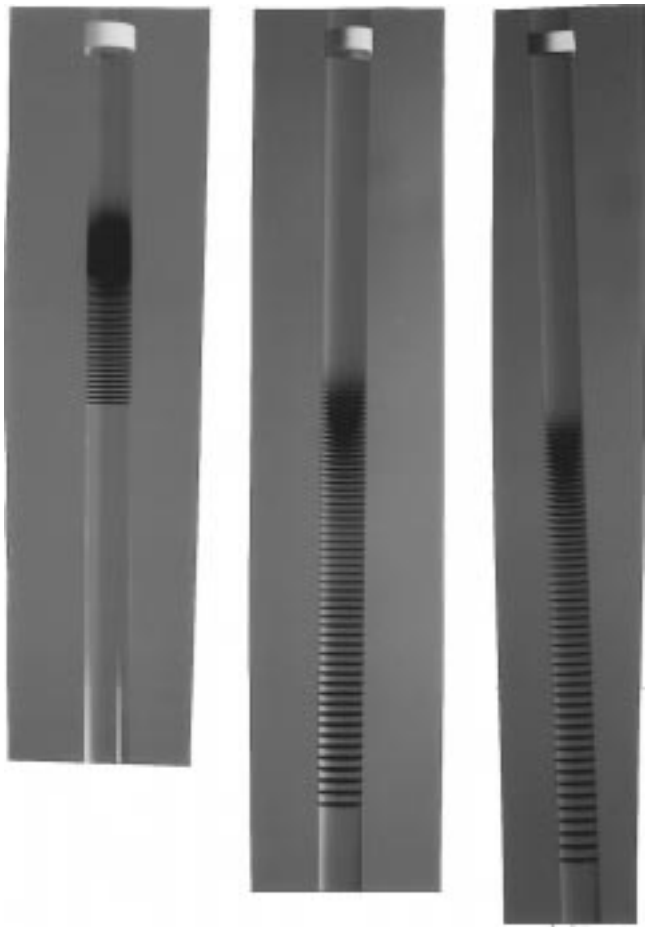

Figure 1. A pattern of $Co(OH)_2$ bands from $CoCl_2$ and NH_4OH. The sequence form left to right shows the propagation of the pattern down the tube. The band dissolution at the top results in a fuzzy appearance of the first bands.

4.0 mm diameter) clamped in a vertical position. The surface of the gel in each tube is marked to indicate the junction between the two coprecipitate solutions. The tubes are covered with Parafilm paper and allowed to stand for 1 day. Then, 1.50 mL of concentrated ammonium hydroxide are added using a graduated pipet, on top of the solidified cobalt chloride gel. The tubes are covered again and allowed to stand. The blue $Co(OH)_2$ bands appear within the first day. A picture of the propagating pattern is depicted in Figure 1. Five tubes with five different initial concentrations (C) of $CoCl_2$ are prepared, using the same amount of gelatin. For a detailed procedure, see ref 1. The concentrations of $CoCl_2$ used are 0.101, 0.134, 0.168, 0.210, and 0.252 M. These values are chosen to test the chaotic property over a range of concentrations, and to study the dependence of the propagation velocities on concentration.

The experiments require a careful control of the conditions, notably the temperature. To achieve this goal, two thermostats (Haake G and D1 models) are used interchangeably because of the long duration of the experiment (40 consecutive days). This provides water circulation into a jacket surrounding a specially designed tube. The tube is monitored for 40 consecutive days, with three observations made per day: at 7.00 a.m., 3.00 p.m., and 11.00 p.m.; these are then converted to time in days. The hours were chosen in a way to ensure a fixed interval of time (8 h) necessary for the analysis of chaotic data. Each observation consists of the following:

a. Measuring the distance of the last band from the interface by means of a ruler to the nearest 0.05 cm (this serves as a reference point).

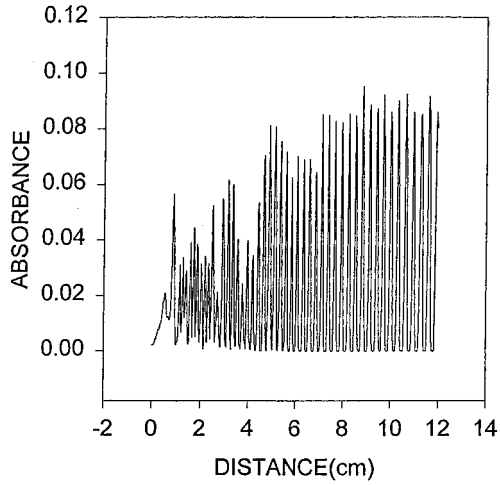

Figure 2. Map of absorbance versus distance from the junction between the two electrolytes obtained by the method descirbed in section 2.2. Each peak with $A > 0$ corresponds to a band of $Co(OH)_2$.

b. Taking a photograph of the whole pattern using a Kodak Digital Science DC50 zoom camera. With this, two additional measurements are performed at each time: the total number of bands N, as the identification of the first band becomes now possible (by image analysis as explained below), and the distance of this first band from the interface.

The identity and the position of the first band could not be determined visually because the latter appeared to be fuzzy at the top of the pattern, as a result of band dissolution (see Figure 1). A criterion is thus needed for deciding on the first band and hence counting the number of bands. A special method of analysis is developed for that purpose, whose details are described in the next section.

2.2. Image Analysis. Each experiment consists of monitoring a tube with a fixed concentration of $CoCl_2$. During each observation one photo is taken, which is then transferred from the digital camera directly to the computer and is saved as an image file. The image is then processed through image analysis software (SigmaScan, Jandel Scientific Software[16]). A criterion based on the absorption of light by the bands formed in the pattern is adopted as follows: the colored picture is transformed into a gray scale image, where the absorbance of each band is characterized. The range of absorbances is then scanned to determine a threshold absorbance value above which the zone is counted as a band. Any value of absorbance less than or equal to this threshold would mean that no band is present. To determine the threshold value, we choose the lowest region near the end of the tube, which contains only cobalt chloride and gelatin with no bands formed or even traces of precipitate present. This region yields a range of transmittance values, the average of which is set as the threshold (T_o). As the tube is scanned, the transmittance value (T) at each point is measured and transformed to its corresponding absorbance value [$A = -\log(T/T_o)$]. A band at a given location is then considered to exist only if $A > 0$ ($T < T_o$). The absorbance is plotted versus position in centimeters. A sample plot is shown in Figure 2. The number of peaks in the plot corresponds to the total number of precipitate bands N in the pattern. A distance calibration is also performed on the image. An axis is drawn parallel to the vertical tube, and the interface between the two solutions is placed at the origin. The distance of the last band to the interface is assigned a reference value (in arbitrary units), chosen as 10 for convenience. With the whole pattern scanned from the interface (origin) to the last band, the positions of all points are

determined in arbitrary units. The latter are then converted to centimeters by means of a scaling factor, since the position of the last band from the junction (in cm) was determined in a separate measurement. This procedure is repeated for all the measurements taken at regular intervals of one-third of a day. The distance of the first peak in the plot (corresponding to the first band in the pattern) can now be determined rigorously. Two major goals are thus achieved by this analysis:

a. A time series is available for chaos characterization of the variable *N*.

b. The distances of the first and the last band from the interface at a given time are determined. As a result, the rate of band dissolution at the top and the rate of band precipitation at the bottom as the pattern progresses down the tube can be measured.

3. A Chaotic Dynamical Variable

The temporal evolution of the total number of bands *N* is determined for five different concentrations of the inner electrolyte cobalt chloride. For each concentration a total of 120 data points are taken. It has been previously shown that *N* displays a random variation with time. Our aim is to characterize this behavior quantitatively and to investigate whether the nonperiodic behavior is due to the inherent dynamics, or to stochastic factors. For this purpose, the software Chaos Data Analyzer[17] (CDA) is used to analyze the data. This tool detects chaos if present in seemingly random data, analyzing and correlating corresponding data points. For the Co^{2+}/NH_4OH system under investigation, only 120 data points are analyzed using CDA. This is relatively a very small number of data points for chaotic data analysis and is due to the extreme slowness of the phenomenon compared with other systems of study. Another reason for this choice is that the pattern of $Co(OH)_2$ bands is stable for only about 40 days (the gel starts breaking), thus making it impossible to obtain more data points. The 120 data points are therefore assumed to be sufficient and representative, given the time scale of the evolution of the pattern. This argument is addressed in more detail in the discussion. The chaos characterization tools used here notably include the calculation of power spectra, Lyapunov exponents, and fractal dimensions.[17] Figure 3 shows the time series (*N* versus time *t*) for the five different concentrations of cobalt chloride. In all concentrations an apparent chaotic behavior is obvious.

The power spectrum is a representation of the Fourier transform performed on the data record, displaying the power *P* (mean square amplitude) as a function of frequency. The frequency is in units of the Nyquist critical frequency (the reciprocal of twice the interval between the data points). The power spectrum is in arbitrary units. Figure 4 (a and b) shows the power spectra for the 0.101 and 0.168 M concentrations. The broad peaks at frequencies 0.31 and 0.24 for those two concentrations, respectively, seem to indicate chaos especially that the spectra have essentially the same shape.

Another tool used here for the analysis of the data as a probe of chaos is the Lyapunov exponent. The *i*th one-dimensional Lyapunov exponent is defined[18] by

$$\lambda_i = \lim_{t\to\infty} \frac{1}{t} \log_2 \frac{p_i(t)}{p_o(t)} \qquad (1)$$

where $p_i(t)$ is the length of the principal axis of the *i*th ellipsoid emerging from an infinitesimal sphere of initial conditions. It is a measure of the rate at which nearby trajectories stretch or shrink.[15,18] The λ_i's are ordered from largest to smallest. Chaotic

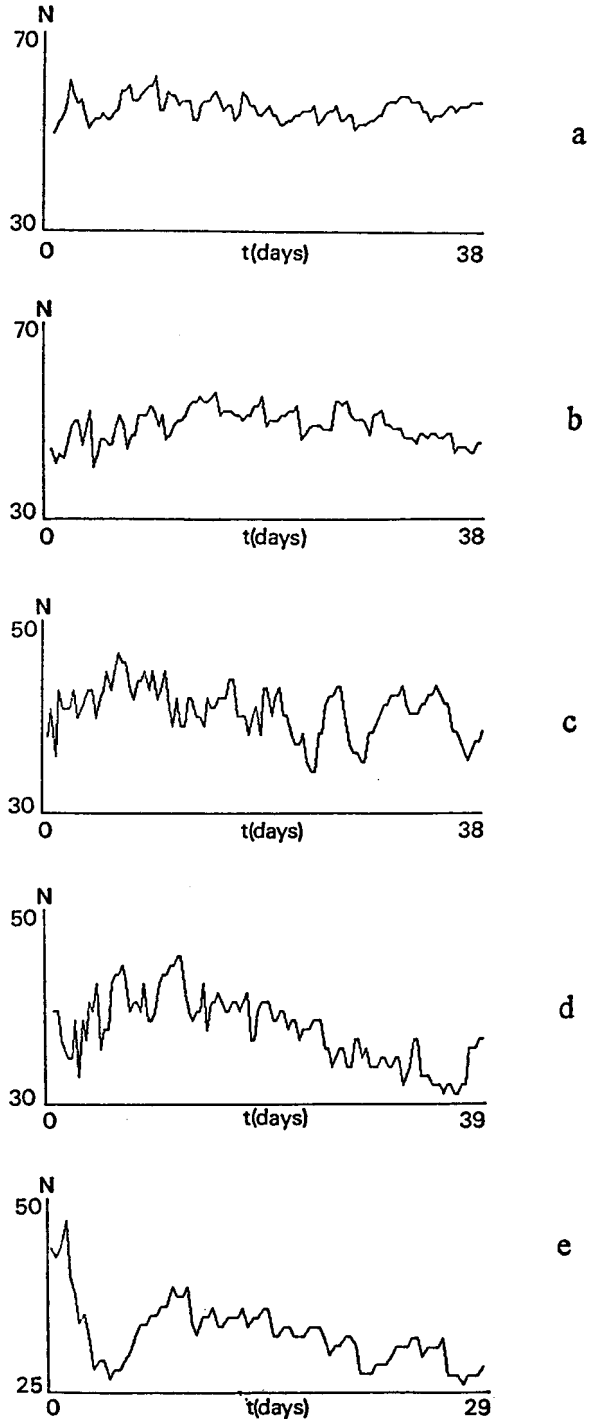

Figure 3. Chaotic time series for the total number of bands *N* at different initial concentrations (*C*) of cobalt chloride: (a) $C = 0.101$ M; (b) $C = 0.134$ M; (c) $C = 0.168$ M; (d) $C = 0.210$ M; (e) $C = 0.252$ M.

(or *strange*) attractors have their largest Lyapunov exponent positive. Figure 5 shows a calculation of the largest Lyapunov exponent (here for the 0.168 M concentration), performed according to the method of Wolf et al.[18] The plot shows the separation in units of the diameter of the smallest *d*-dimensional hypersphere that encloses the attractor at *n* successive time steps. The parameter *n* is the number of sample intervals over which a pair of points is followed before a new pair is chosen (here we see that $n = 3$). The positive value of 0.434 (bits/data sample) for λ_1 is suggestive of deterministic chaos.

Another important tool for the analysis of our data is the correlation dimension. A reference point is chosen for the data,

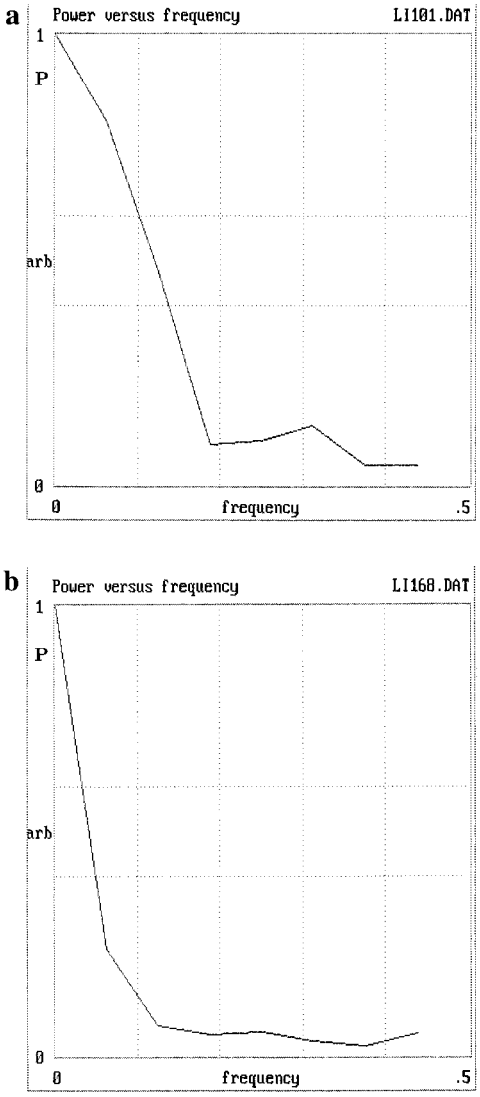

Figure 4. Power spectra (power *P* versus frequency) for (a) 0.101 M and **(**b) 0.168 M concentrations. The similarities in the broad peaks at frequencies 0.31 and 0.24, respectively, seem to indicate a deterministic trend.

and all the distances from this point to the $N - 1$ remaining points are computed. The number of data points within a hyperdimensional sphere of radius r centered at the reference point can then be computed. The correlation function $C(r)$ measures the extent to which the presence of a given data point affects the position of all other points; it is defined[19] by the relation

$$C(r) = \frac{1}{N^2} \sum_{i,j=1,i=j}^{N} \theta(r - |\chi_i - \chi_j|) \qquad (2)$$

where χ_i is a point of phase space and θ is the Heaviside function. For a d- dimensional manifold, $C(r)$ is proportional to r^d. Thus the dimensionality d of the attractor is given by the slope of the plot of ln $C(r)$ versus ln r (because ln $C(r)$ = d ln(r) + k). Figure 6 shows such a plot for the 0.210 M concentration. It is clearly seen that the points fall on a smooth curve. The noninteger value of d (3.090) suggests the fractal nature of the attractor. Note that a dimension greater than about 5 implies that the observed nonperiodic behavior is not chaotic but is merely stochastic.

Phase portraits are finally depicted in Figures 7 and 8. Figure 7 shows the plot of the time derivative of N versus N at each data point (this is often done for systems where one variable is involved). Frames a and b correspond to the 0.168 and 0.210 M concentrations, respectively. Figure 8 shows the corresponding plots of $N(t)$ versus $N(t - 1)$. Both plots yield strange attractors of fractal dimensions 3.628 and 3.090 for the 0.168 and 0.210 M concentrations, respectively.

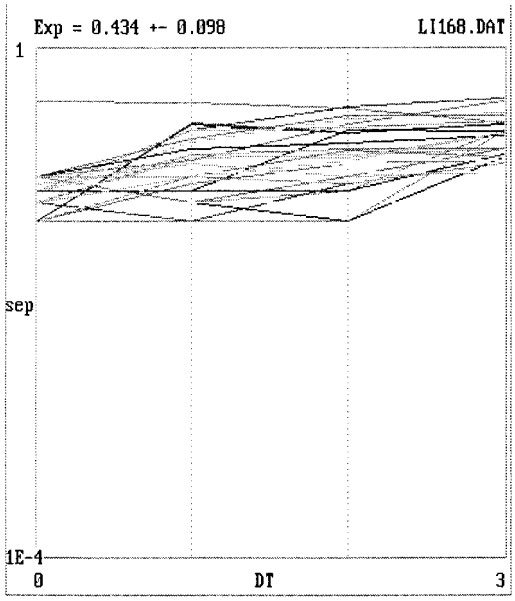

Figure 5. Largest Lyapunov exponent estimated by following the evolution of chosen pairs of data points shown here for the 0.168 M concentration. Each line represents the evolution of a pair. The number of time intervals between consecutive chosen pairs of points, $n = 3$. $\lambda_1 = 0.434$ bits/data sample. $\lambda_1 > 0$ suggesting chaos.

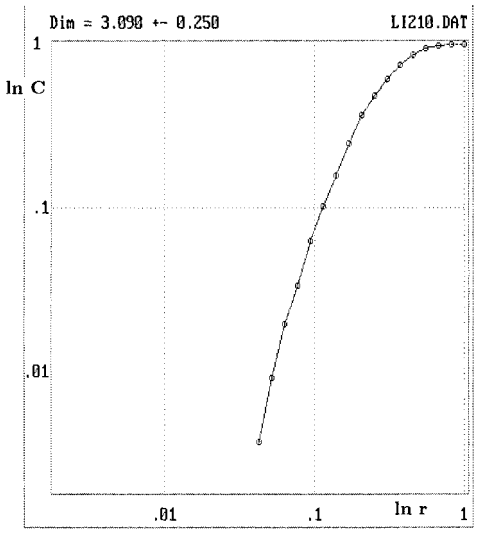

Figure 6. Correlation dimension for the 0.210 M concentration. The fractal dimension obtained ($d = 3.090$) reveals the chaotic nature of the data. The plot shows the log of the number of points within a sphere versus the log of the sphere's radius.

All the tools used for the analysis of the random data obtained, apparently suggest a chaotic behavior. This evidence reveals a chaotic dynamics inherent in the nature of the propagating $Co(OH)_2$ pattern, thus making the Co^{2+}/NH_4OH system a unique Liesegang system with very interesting features.

4. Dissolution and Precipitation Fronts

When the concentrated ammonia solution is added on top of the gel solution of cobalt chloride, a homogeneous blue solid

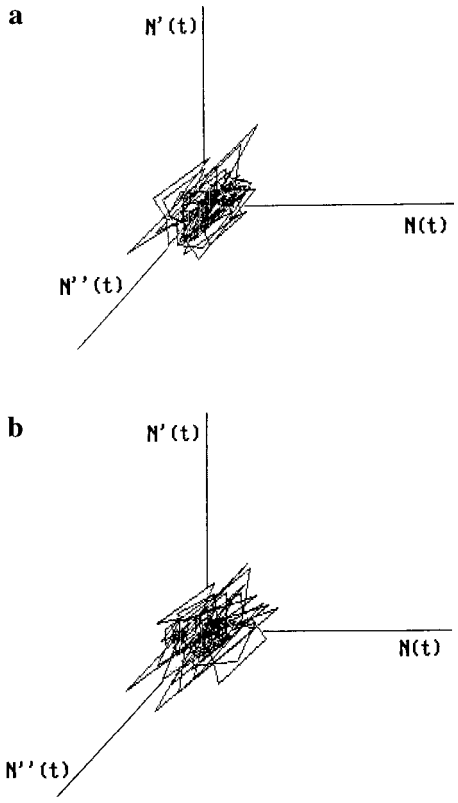

Figure 7. Phase-space plots (phase portraits) in three dimensions (showing $N(t)$ versus $N'(t)$ versus $N''(t)$) yielding strange attractors: (a) $C = 0.168$ M; (b) $C = 0.210$ M.

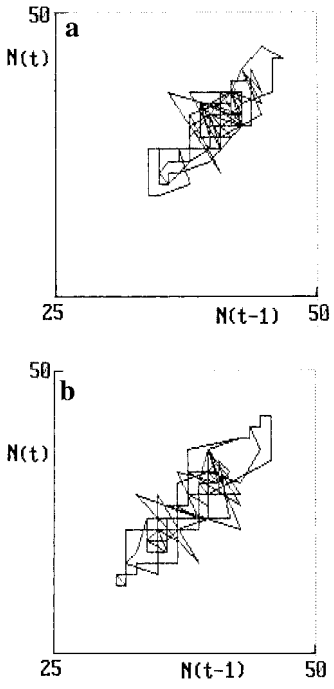

Figure 8. Phase portraits, choosing time delays of one time interval (0.333 day). The obtained strange attractors resemble those of other known chaotic data. Frames a and b are the same as in Figure 7.

forms at the interface. Liesegang bands start to appear within the first day. The dissolution of the blue $Co(OH)_2$ bands at the top of the pattern and the appearance of new ones at the bottom as time advances leads to a propagating pattern of bands. This migration of the whole pattern becomes noticeable about 2 days after the start of the reaction. The precipitation front propagates just behind the diffusion front of OH^- and its velocity provides

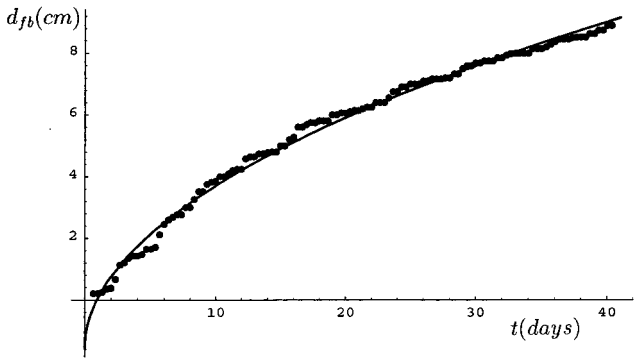

Figure 9. Variation of the distance of the first band d_{fb} at $C = 0.168$ M with time in days. The points are experimental measurements. The solid curve is a computer (square root) fit. The velocity is obtained by calculating the derivative at a given point. Note that the velocity decreases as time advances since the slope of the curve becomes smoother.

a measure of the coupling of the diffusion and reaction processes. Call the velocity of the dissolution front V_{diss} and that of the precipitation front V_{prec}. The velocities and their temporal variation directly affect the time dependence of the total number of bands N. It is this dissolution/precipitation repetitive cycle that yields the oscillatory behavior observed in the time series (Figure 3). Note that velocities of pattern advancement in Liesegang systems were previously measured[6,8] using monitoring techniques similar to the ones described below. The novel feature here lies mainly in the dissolution phenomenon and its probable correlation to the diffusion−precipitation fronts, causing the whole pattern to move downward. To determine front velocities, the temporal evolution of the distance of the first band and that of the last band are measured. The distance of the first band from the junction (d_{fb}) is determined as accurately as possible using the image analysis described in section 2.2. The difficulty lies in that the top bands are faint (because of dissolution) and require a quantitative criterion to count or not count a band. The location of the first band is monitored with time for 40 consecutive days, three times per day. A plot of d_{fb} versus time (t) shows a monotonically increasing curve, essentially fitting a square root-type dependence, as shown in Figure 9. Similar square-root profiles were obtained in other Liesegang systems, such as pH fronts and colloid turbidity fronts in $Mg(OH)_2$ patterns[8] and precipitation fronts in PbI_2 patterns.[20] The plot in Figure 9 provides a measure of the motion of the first band away from the junction as time advances, due to the dissolution of bands at the top of the pattern. The velocity of the dissolution front is determined by first obtaining a functional fit from the time variation curve (solid line). A reference day is chosen (say, $t = 10$ days). A derivative of the d_{fb} versus t curve can then be calculated at all points and is particularly evaluated at $t = 10$ days. Note that the velocity decreases as the pattern moves down the tube, as indicated by the slope of the d_{fb} versus t curve—the latter becomes smoother as t advances. The distance of the last band from the junction (d_{lb}) is measured manually using a ruler because of its distinct appearance. A plot of d_{lb} versus t shows a montonically increasing curve, similar to the previous one, as seen in Figure 10. As expected, the last band also becomes farther away from the junction as time advances. Note that the d_{lb} versus t curve is much sharper and clearer than the d_{fb} versus t plot because of the sharpness of the last band and the smaller uncertainty in its location. Figure 11 shows a plot of the distance of the last band (d_{lb}) versus the distance of the first band (d_{fb}). We see that the correlation between these two variables is

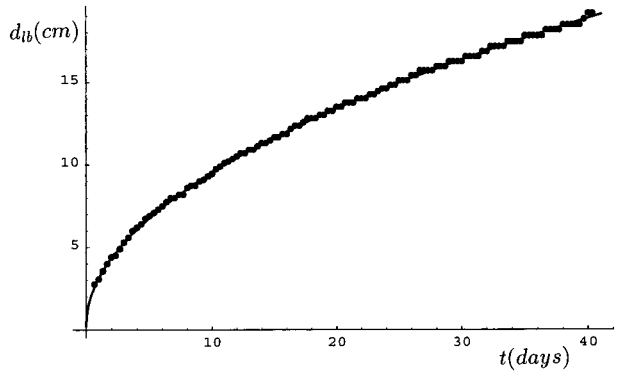

Figure 10. Variation of the distance of the last band d_{lb} at $C = 0.168$ M with time in days. The velocity calculation is the same as in Figure 9.

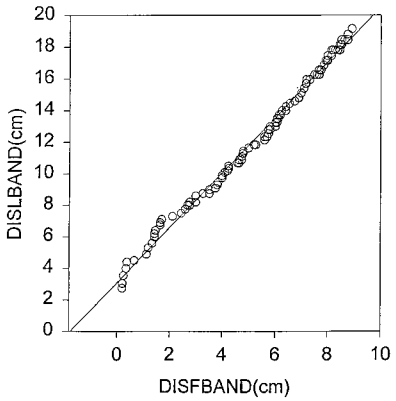

Figure 11. Correlation plot of d_{lb} versus d_{fb} for $C = 0.168$ M. The correlation is essentially linear revealing a concerted mechanism.

essentially linear. It is because of this linear correlation that we adopt the same functional fit (a square root form) for the temporal variation of the two distances d_{lb} and d_{fb}. The dependence of the front velocities on the concentration of cobalt chloride at a fixed time is investigated. For this purpose, different concentrations of cobalt chloride are used: 0.101, 0.134, 0.168, 0.210, and 0.252 M. The whole experiment is repeated for each concentration (each experiment spanning 40 days). The velocity (for both dissolution and precipitation) is extracted at two representative times ($t = 10$ and 15 days) for each concentration, as described above. Then the latter velocity (V_{diss} or V_{prec}) is plotted versus $[CoCl_2] = C$. The results are shown in Figures 12 and 13. The units of the front velocities are expressed in centimeters traveled by the front per day (cm/day). We see that both the dissolution and precipitation velocities decrease monotonically with increasing concentration of the inner electrolyte. A linear correlation is also found to exist between V_{prec} and V_{diss} when the former is plotted versus the latter, as depicted in Figure 14. This result is particularly interesting since it points out the coherence of the phenomenon and the concerted character of the processes taking place at the top and the bottom of the pattern. The correlation of events reveals a coherent dynamics that supports the observed chaos as apparently emerging from an overall self-contained mechanism.

5. Conclusions and Discussion

The main results of the present study may now be summarized as follows:

1. The diffusion of an NH_4OH solution into a gel containing Co^{2+} yields a Liesegang pattern of parallel blue $Co(OH)_2$ bands that propagates down the tube.

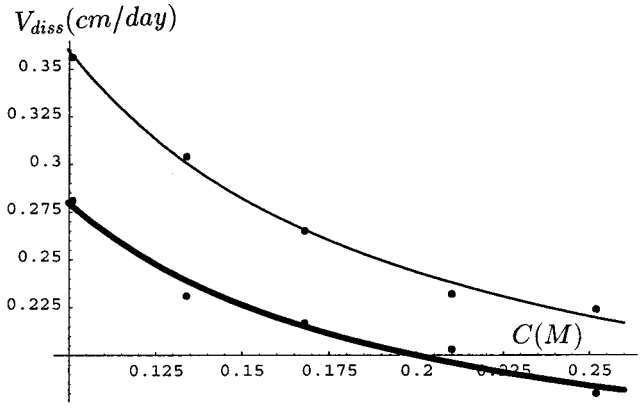

Figure 12. Dependence of the dissolution velocity V_{diss} on the concentration of $CoCl_2$: (thin line) $t = 10$ days; (thick line) $t = 15$ days. Each point is obtained from a 40 day experiment. The velocity of the dissolution front is shown to decrease monotonically with concentration (C).

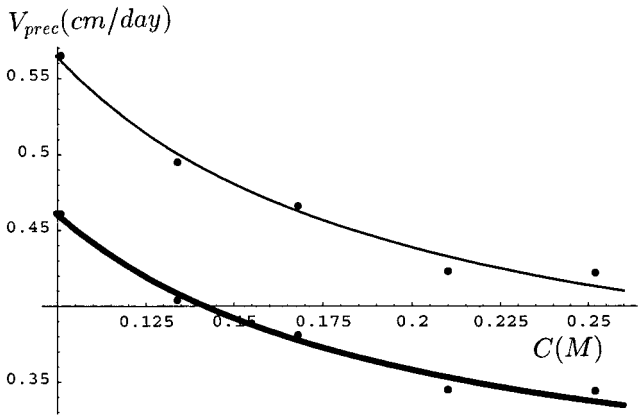

Figure 13. Dependence of V_{prec} on the concentration of $CoCl_2$: (thin line) $t = 10$ days; (thick line) $t = 15$ days. The velocity of the precipitation front decreases monotonically with C.

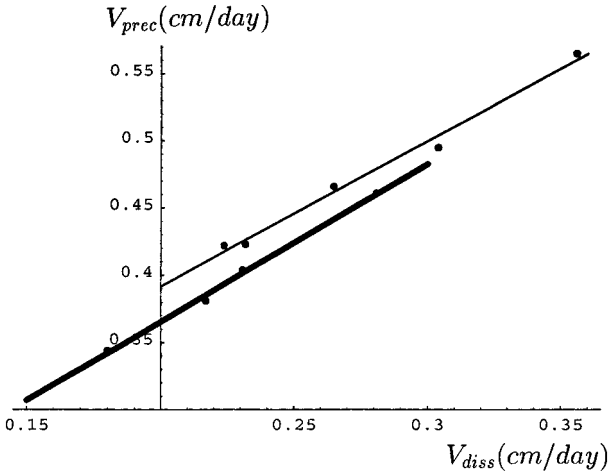

Figure 14. Correlation plot of V_{prec} versus V_{diss} at $t = 10$ days (thin) and $t = 15$ days (thick). The linear correlation reveals a coherent dynamics supportive of the idea of deterministic chaos.

2. The propagation is due to the dissolution of bands at the top of the pattern (because of complexation with ammonia) and the formation of new ones by precipitation at the bottom.

3. The velocities of the dissolution and precipitation fronts (V_{diss} and V_{prec}) are measured, and the variation of those velocities with the concentration of Co^{2+} in the gel is determined at two representative times ($t = 10$ and 15 days). Both V_{diss} and V_{prec} decrease monotonically with concentration. The

correlation between the two velocities is linear, suggesting a concerted mechanism.

4. The erratic variation of the total number of bands (N) with time is characterized as a situation of deterministic chaos inherent in the dynamics of the diffusion−precipitation−dissolution scenario.

Although the characterization is based on a short time series (a maximum of 120 data points), it is nevertheless revealing based on the tools used and a set of other important observations discussed here. A basic deterministic feature observed in our experiments is the reproducibility in the band locations. A variation in the latter parameter from one experiment to the other under the same conditions would constitute a distinct stochastic element.[21,22] The reproducibilty in the band locations observed here (and hence the reliabilty of the velocity measurements) ascribes the oscillations in the variable N to a dynamics other than stochastic.

The linear correlation between d_{fb} and d_{lb} seen notably in Figure 11 is also an argument in favor of determinism since it reveals a certain extent of "synchronization" between the events at the top and the bottom. A comparison between the strange attractors in Figures 7 and 8 and phase portraits of other systems with short time series believed to be chaotic reveals significant similarities. The irregular and sharp segments capture the features of phase portraits[19] representing the climatic evolution over the last one million years, inferred from the time series of $^{18}O/^{16}O$ isotope data of deep sea core sediments. Correlation functions of those climatic attractors were calculated, yielding plots similar to those of Figure 6 and comparable correlation dimensions. Similar properties are found[14] in strange attractors for the Great Salt Lake volume fluctuations. Chaos analysis of short time series is often applied in biological systems[23,24] in an attempt to establish a dynamical regime for the evolution of various species populations. Transition to chaos was demonstrated in the population of the flour beetle *tribolium*.[24] The tools used included a calculation of Lyapunov exponents for a time series that counted only 40 data points. The chaotic dynamics was further supported by matching predictions emerging from a nonlinear demographic model. This brings a suggestion for the next study to probe our chaotic dynamics obtained by standard diagnostic analyses of time series residuals: the attempt to predict the observed dynamics by a mathematical model incorporationg the coupling of diffusion, precipitation, and dissolution. Such a model is under present investigation.

Acknowledgment. This work was supported by a Bobst start-up and a URB research grant (American University of Beirut).

References and Notes

(1) Sultan R.; Sadek S. *J. Phys. Chem.* **1996**, *100*, 16912.
(2) Liesegang, R. E. *Lieseg. Phot. Archiv.* **1896**, *21*, 221. Liesegang, R. E. *Naturewiss. Wochenschr.* **1896**, *11*, 353.
(3) Hedges, E. S. *Liesegang Rings and Other Periodic Structures*; Chapman and Hall: London, 1932.
(4) Stern, K. H. *Chem. Rev.* **1954**, *54*, 79. *A Bibliography of Liesegang Rings*, 2nd ed.; Government Printing Office: Washington, DC, 1967.
(5) Henisch, H. K. *Crystals in Gels and Liesegang Rings*; Cambridge University Press: Cambridge, U.K., 1988.
(6) Jablczynski, C. K. *Bull. Soc. Chim. Fr.* **1923**, *33*, 1592.
(7) Morse, K.; Pierce. *Z. Phys. Chim.* **1903**, *45*, 589.
(8) Kai, S.; Müller, S. C.; Ross, J. *J. Chem. Phys.* **1982**, *76*, 1392.
(9) Müller, S. C.; Kai, S.; Ross, J. *J. Phys. Chem.* **1982**, *86*, 4078.
(10) Zrínyi, M.; Gálfi, L.; Smidróczki, É.; Rácz, Z.; Horkay, F. *J. Phys. Chem.* **1991**, *95*, 1618.
(11) Das, I.; Pushkarna, A.; Agrawal, N. R. *J. Phys. Chem.* **1989**, *93*, 7269.
(12) Ostwald, W. *Kolloid Z.* **1925**, *36*, 380.
(13) Lloyd, F. E.; 'Moravek, V. *Plant Physiol.* **1928**, *3*, 101.
(14) Abarbanel, H. D. I. *Analysis of Observed Chaotic Data*; Springer: New York, 1996.
(15) Abraham, N. B.; Gollub, J. P.; Swinney, H. L. *Physica D* **1984**, *11*, 252.
(16) *SigmaScan*; Jandel Scientific Software: San Rafael, CA, 1995.
(17) Sprott, J. C.; Rowlands, G. *Chaos Data Analyzer*; Physics Academic Software, AIP: New York, 1992.
(18) Wolf, A.; Swift, J. B.; Swinney, H. L.; Vastano, J. A. *Physica D* **1985**, *16*, 285.
(19) Nicolis, G.; Prigogine, I. *Exploring Complexity*; W. H. Freeman: New York, 1989.
(20) LeVan, M. E.; Ross, J. *J. Phys. Chem.* **1987**, *91*, 6300.
(21) Kai, S.; Müller, S. C.; Ross, J. *J. Phys. Chem.* **1983**, *87*, 806.
(22) Attieh, M.; Al-Kassem, N.; Sultan, R. *J. Chem. Soc., Faraday Trans.* **1998**, *94*, 2187.
(23) May, R. M. *Science* **1974**, *186*, 645.
(24) Costantino, R. F.; Desharnais, R. A.; Cushing, J. M.; Dennis, B. *Science* **1997**, *275*, 389.